

Flexural Behaviour of Concrete Beams Reinforced with Fiberglass Geogrid

Mohamed Shokr^{1}, Mohamed Meguid¹, Sam Bhat², and Deniele Malomo¹*

¹Department of Civil Engineering, McGill University, Canada

²VP Global Business Development & CTO Geosynthetics, Titan Environmental Containment Ltd, Canada

Abstract. In cold regions, especially within Canada, the degradation of non-structural concrete components in challenging environmental conditions has become a pressing issue. Traditional steel reinforcements are known to be susceptible to corrosion. With anticipated climate shifts causing variations in temperature, precipitation, and freeze-thaw cycles, there's an increasing need for more resilient reinforcement materials to deter premature cracking in non-structural concrete components. This study delves into the advantages of using low-ductility fiberglass geogrids as reinforcement layers to curb crack development and augment the flexural performance of plain concrete beams. Tests were carried out on nine concrete beams, each measuring 550×150×150 mm, with diverse reinforcement setups. The emphasis was on evaluating load-deflection characteristics, energy absorption capabilities, and modes of failure. Results suggest that low-ductility fiberglass geogrid reinforcement markedly enhances the flexural strength of plain concrete, outperforming control beams. Additionally, fiberglass reinforcement showcases enhanced crack resistance and post-cracking behaviour than plain beams. A Finite Element Analysis (FEA) was also executed using the Abaqus software, and its accuracy was confirmed through experimental data comparisons, yielding numerical figures for mid-span deflection and peak load. This research furnishes pivotal insights into the prospective use of progressive reinforcement materials to combat environmental challenges in colder climates.

1 Introduction

Traditional steel mesh or bars are commonly employed to enhance the durability of Portland cement concrete pavements, enabling them to withstand the pressures exerted by traffic loads. However, despite the fundamental improvements they provide, there are limitations to their utilization. These limitations include concerns about steel corrosion due to chemical reactions and challenges associated with placing reinforcing steel bars in thin sections, such as concrete

* Corresponding author: mohamed.shokr@mail.mcgill.ca

pavement overlays. Moreover, alternative reinforcement materials like fibre-reinforced polymer bars and grids are gaining prominence as substitutes for traditional steel reinforcement.

In light of steel limitations, various research endeavours have been undertaken to explore the use of polymeric geogrid as reinforcements for concrete elements. In a study by Tang (2008), both rigid and flexible biaxial geogrids were utilized to reinforce Portland cement concrete beams, under four-point bending tests. Results demonstrated that geogrids enhanced post-cracking ductility and flexural strength, with stiffer reinforcements outperforming flexible ones [1]. Additional research by El Meski (2014) and Pavithra (2022) evaluated geogrid reinforcement's mechanical impact on concrete overlays using various geogrid configurations, finding improved ductility, load-bearing capacity, and deflection resistance in geogrid-reinforced concrete beams compared to unreinforced specimens [2, 3]. Al Masri (2018) compared plain concrete beams to biaxial geogrid-reinforced ones using direct tension and four-point flexural bending tests, indicating a 130% higher load capacity and better post-cracking ductility in reinforced beams, suggesting geogrids as steel replacements for ground concrete applications [4]. Itani (2016) investigated uniaxial geogrid-reinforced concrete's crack control performance, revealing a 25% higher tensile strength, superior post-cracking ductility, and improved crack control performance compared to plain concrete [5].

In recent experiments conducted by Al-Hedad Abbas in 2019 and Rajesh Kumar in 2021, the influence of geogrid reinforcement on concrete slabs was assessed [6, 7]. Al-Hedad Abbas employed triaxial geogrid layers for reinforcement, while Rajesh Kumar compared the performance of steel-reinforced and geogrid-reinforced concrete slabs. Both studies concluded that the use of geogrids led to a notable improvement of at least 15% in flexural strength and enhanced crack resistance in concrete slabs [6, 7]. Additionally, Al-Hedad (2017) utilized 13 strain gauges to measure surface strain in control slabs and those reinforced with a triaxial geogrid layer positioned approximately 17 mm from the bottom, finding significant enhancements in flexural strength due to the presence of geogrids [8]. Notably, the mechanical properties of the geogrids were identified as pivotal factors in the reinforced concrete's performance, with stiff geogrids consistently yielding superior results. Building upon these prior findings, this study explores the mechanical contribution of stiff fibreglass geogrids as a novel reinforcement for non-structural concrete. It investigates the flexural performance of fibreglass-reinforced concrete beams by comparing them with plain concrete specimens.

2 Experimental program and results

2.1 Testing program and materials

The experimental campaign encompassed nine beams categorized into three groups. The first category comprised the control specimens where no reinforcement was used. In the second and third categories, fibreglass reinforcement was tested at depths of 15 mm and 45 mm, respectively. The nine concrete beams were constructed using a type I Portland cement concrete mix, along with ¼" coarse aggregate, ½" coarse aggregate, and sand. The coarse aggregates to medium aggregate to sand to cement proportions by mass were 0.42: 1.17: 1.16: 1 with a water-cement ratio of 0.4. Notably, the maximum aggregate size was deliberately chosen to be smaller than the geogrid aperture dimensions, ensuring larger aggregates could easily pass through.

Furthermore, the concrete mix possessed an average slump of 120 mm, promoting effective contact and interlocking between the aggregates and geogrids. Following the

mixing process, the concrete was poured into moulds and allowed to cure for a duration of 28 days before undergoing testing. Additionally, eight separate concrete cylinders were subjected to compressive and tensile split tests according to ASTM C 39 and C 496, respectively, resulting in nominal strengths of 30MPa and 3MPa, with a coefficient of variance of 1.7 and 2, respectively [9, 10].

The material properties of the low-ductility fibreglass geogrid were obtained from recent research by Shokr et al. (2021), as shown in Figure 1 [11]. At room temperature, the fibreglass geogrid exhibited an ultimate tensile strength of 105 kN/m and an ultimate strain of 2%. All samples in this study were sourced from the same roll of this particular geogrid material.

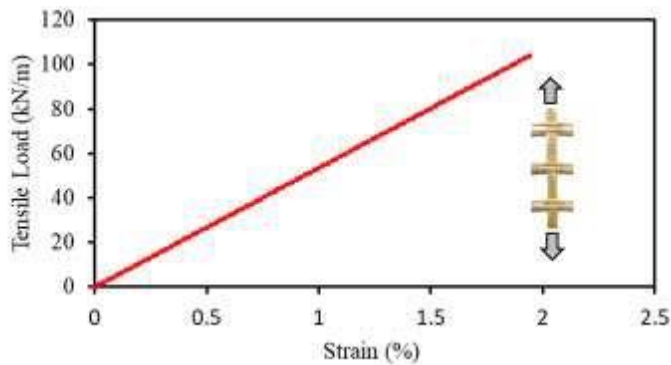


Fig. 1. Tensile load-strain curve of fibreglass geogrid adopted from Shokr et al. (2021)

2.2 Testing program and materials

Nine wooden moulds, measuring 550×150×150 mm, were prepared and filled with the first layer of concrete. A vibration table was used to consolidate the concrete and create a smooth surface. A 55×15 cm geogrid sheet was placed precisely at the bottom of each beam, followed by pouring a second batch of concrete and finishing the surface. A rectangular glass notch, 150 mm wide and 15 mm deep, was attached to the mould's bottom at its midpoint. The concrete for all specimens was prepared in three batches, with each specimen cast from a single batch to minimize variability. Additionally, concrete cylinders were produced to test concrete strength and variability, and the results showed minimal batch-to-batch variability. The concrete specimens were subjected to flexural testing, which involved applying a continuous vertical load at the midpoint of the beam using an MTS machine equipped with a 150 kN load cell, as depicted in Figure 2. The loading was conducted in displacement control mode with a 1.2 mm/min crosshead rate. Prior to each test, a steel ruler was affixed to the top mid-span of the beam. This setup allowed for the placement of two linear variable differential transformers (LVDTs) at each end to measure the displacement at the mid-span, as shown in Figure 2. The four-point bending test was carried out using data acquisition software (Testworks), which recorded data concerning both the applied loads and the vertical mid-span displacements until the point of failure was reached.

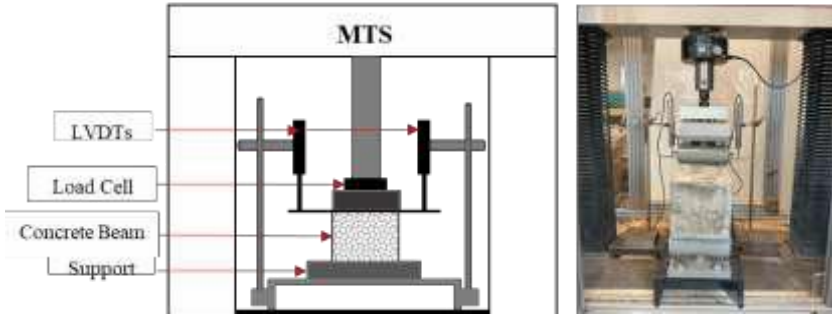


Fig. 2. MTS loading machine for four-point flexural tests

2.3 Testing program and materials

This section presents the test results for different types of concrete beams. Control beams, without reinforcement, experienced brittle failure with a peak load of 25 kN. Fibreglass geogrid-reinforced beams at 15 mm exhibited post-crack behaviour at higher loads, with a 35% increase in peak load compared to the control beams. This improvement in load capacity was attributed to the fibreglass geogrid's high strength and low ductility. Fibreglass geogrid-reinforced beams at 45 mm depth had a similar peak load to the control beam, but the load was redistributed to the geogrid after reaching this point, resulting in further load-carrying capacity until the beam's total failure. The depth of reinforcement plays a key role as the smaller depth allows for a larger amount of tensile reinforcement to resist bending moments and increase the beam's overall strength. The modulus of rupture for each specimen was calculated using the ASTM 2015 equation [12].

$$R = pl/bd^2 \quad (1)$$

In this equation, R represents the modulus of rupture in MPa, P denotes the maximum applied load by the testing machine in N, l stands for the span length in mm, while b and d correspond to the average width and depth of the specimen in mm, respectively. Based on the average of three replicated specimens per set, it has been demonstrated that specimens reinforced with fibreglass geogrid at a depth of 15 mm exhibit an increase in their rupture modulus up to 33% and up to 12% for the specimens with reinforcement at 45 mm, in comparison to control beams.

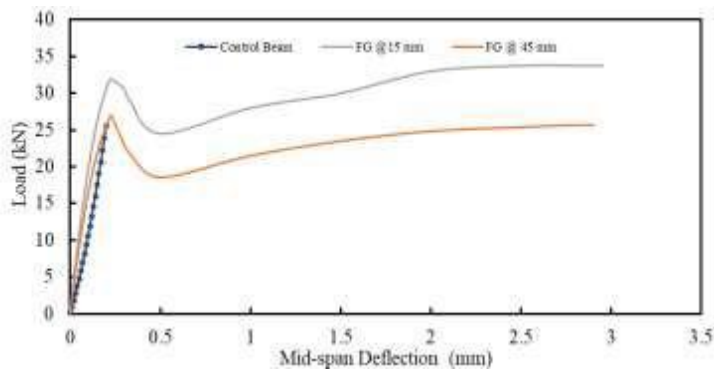


Fig. 3. Load versus mid-span deflection for the three replicate control beams and fibreglass reinforced beams

2.3.1 Fracture energy

Fracture energy serves as a critical parameter in evaluating the fracture characteristics of concrete, providing valuable insights into its crack resistance [13, 14]. While direct tension testing theoretically offers the most precise means of determining concrete's fracture energy, practical limitations arise due to concrete's limited deformation capacity and the stiffness of test specimens. Consequently, alternative methods involving three-point or four-point load tests have become prevalent for evaluating concrete's fracture energy by calculating the area beneath the load-deflection curve [15–18]. A notable improvement in fracture energy is observed when implementing fibreglass geogrid reinforcement in concrete beams, as depicted in Figure 3. Beams reinforced with fibreglass geogrid exhibit a substantial enhancement in fracture energy, ranging from 35% to 60%, compared to control beams. This enhancement is contingent on the reinforcement depth and can be attributed to the superior strength and lower ductility of fibreglass geogrid compared to conventional polymeric geogrids.

2.3.2 Failure mode

Figure 4 provides visual representations of the diverse failure modes observed in each specimen configuration. Control beams, lacking any reinforcement, exhibited brittle failure. In contrast, the fibreglass-reinforced specimens demonstrated ductile behaviour, with the concrete and geogrid working together to absorb the tensile stresses induced by bending. In the Fibreglass geogrid reinforcement, the beam's structural integrity was maintained even after the total failure occurred, with cracks extending to the top of the beams, as evidenced in Figure 5c.



Fig. 4. Failure modes for control and reinforced beams

3 Finite element modelling

3.1 Material model and solution technique

Finite Element Analysis (FEA) was conducted using Abaqus software to simulate experimental data from control and beams reinforced with low ductility fibreglass geogrid. The study involved sensitivity analyses to optimize mesh sizes and step sizes for improved

outcomes. Concrete properties were represented using 8-noded hexahedral elements (C3D8R) capable of simulating cracks in tension and compression zones, while reinforcements were modelled with 2-noded linear truss elements (T3D2). To simplify the modelling process, the combination of fibreglass reinforcement and concrete was achieved using the tie command (Embedded), mirroring the assumption of perfect bonding between internal bars and concrete in theoretical analysis.

Concrete Damage Plasticity (CDP) is a constitutive modelling approach employed in structural engineering to simulate the nonlinear behaviour of concrete under various loading conditions. It's widely recognized for its ability to capture the post-peak softening behaviour of concrete, making it a crucial tool for analyzing and designing structures subjected to complex loading scenarios [19, 20]. The Concrete Damage Plasticity model was initially formulated by Lubliner et al. in the early 1980s and has since undergone various modifications and enhancements by researchers in the field [21, 22]. These modifications have improved the model's accuracy and applicability to a wide range of concrete materials and structural configurations.

The (CDP) model relies on essential parameters such as the viscosity parameter, the dilation angle, the flow potential eccentricity and the ratio of initial biaxial compressive yield stress to initial uniaxial compressive yield stress. Each parameter plays a unique role in accurately describing the behaviour of concrete under various loading conditions. The model was validated using experimental data obtained from control beams. The finite element model consists of two materials: concrete and Fiberglass geogrid reinforcement. The concrete's compressive strength is established at 30 MPa, determined through standard compressive cylinder tests.

Additionally, the modulus of elasticity of concrete (E_c) is calculated using the equation $E_c = 4700 f' c^{0.5}$, as specified by the ACI Code [23]. Furthermore, a Poisson's ratio of 0.2 has been chosen to represent the concrete's elastic response. A dilation angle of 40 was uniformly applied in simulating all specimens as recommended by several researchers [24, 25]. For critical parameters like the yield shape surface, K_c , and eccentricity (ϵ), the Concrete Damage Plasticity (CDP) model recommends values of 2/3 and 0.1, respectively, as per references [26–28].

After conducting sensitivity analyses involving three different maximum increment values (0.01, 0.001, and 0.0001), it was determined that the influence of varying the maximum increment on the results is relatively minor. Consequently, the choice was made to use the maximum increment of 0.01, optimizing computational efficiency. The viscosity parameter was found to substantially impact the load-deflection response of the beam, as highlighted in references [27, 29, 30]. Recommended values for viscosity range from 0 (as suggested by [20, 31]) to 0.5 (as recommended by [27, 30]). Five different values (0.5, 0, 0.01, 0.001, 0.0001) were considered in a sensitivity analysis to explore the effect of the viscosity parameter. Ultimately, a viscosity value of 0.001 was selected due to its superior agreement with the experimental results in terms of ultimate load capacity and load-deflection response.

For modelling the fibreglass response, an isotropic linear elastic response was adopted within Abaqus without implementing any damage criteria until the point of failure. This choice of linear elastic behaviour for fibreglass geogrid was made because it typically exhibits a brittle failure mode after reaching its yield point without undergoing plastic deformation. This modelling approach aligns with recommendations found in several research studies addressing the behaviour of GFRP (Glass Fiber Reinforced Polymer) bars, which share similarities with fibreglass geogrid in terms of their brittle and elastic characteristics [32–35]. It's essential to emphasize that both fibreglass geogrid and GFRP are classified as brittle materials characterized by their elastic behaviour. The final numerical model is shown in Figure 5.

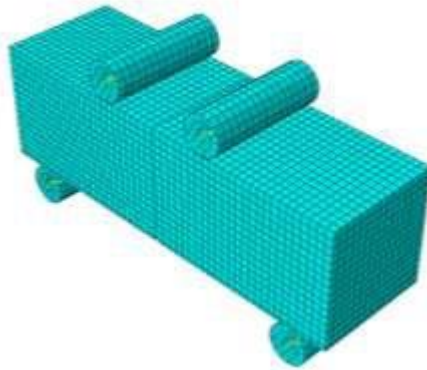


Fig. 5. The 3D FE mesh for the concrete beam

3.2 Results

The Abaqus techniques were used to simulate both the control beam and the Fiberglass geogrid-reinforced concrete beam at 15 mm and 45 mm depths, as described in the previous section. This section aims to validate the numerical modelling method by comparing the simulation results with the experimental findings. Figures 6 and 7 provide the ultimate load and corresponding displacement data for the three beam configurations, as obtained through simulation and experimentation, respectively. In the case of the control beam configuration, the Finite Element Analysis (FEA) shows a slightly stiffer response compared to the experimental results, which could be attributed to microcracking of the beam before testing. However, for the other reinforced configurations, the Finite Element simulation demonstrates a good agreement, with differences ranging from 3% to 12% when compared to the experimental results in terms of ultimate load and corresponding displacement. It's important to note that the failure mode observed in the simulation aligns with the failure mode in the experiment. This alignment was crucial to the Finite Element calibration process, enhancing the model's reliability.

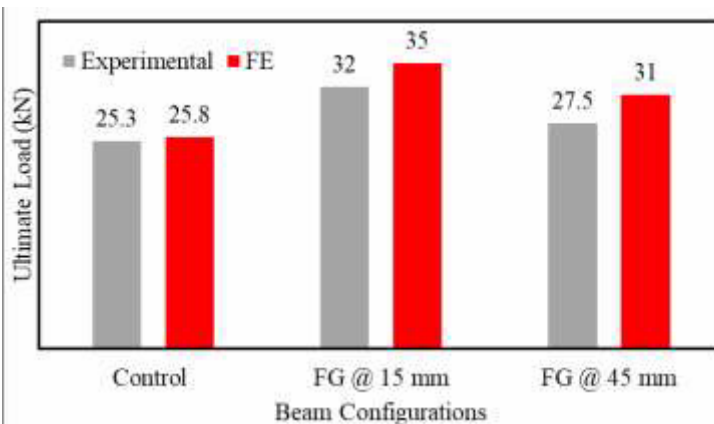


Fig. 7. Ultimate loads for all beam configurations for experimental and FE analysis

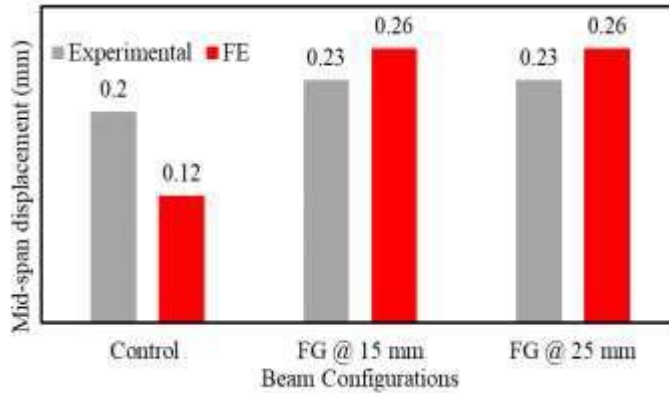


Fig. 8. The corresponding displacements for all beam configurations for experimental and FE analysis

4 Conclusions

This study presents the findings of an experimental and numerical investigation into the flexural behaviour of concrete beams reinforced with low-ductility fibreglass geogrids. A total of nine concrete beams were meticulously prepared and subjected to four-point bending tests. The outcomes of these beam flexure tests underscore the advantages of employing geogrid reinforcement in concrete beams. Both geogrid reinforcement configurations at 15 mm and 45 mm depth demonstrated ductile post-cracking behaviour, increased deflection capacity, and elevated fracture energy compared to unreinforced beams. Moreover, Fibreglass geogrid-reinforced beams at 15 mm exhibited post-crack behaviour at higher loads, with a 35% increase in peak load compared to the control beams. It is essential to emphasize that the physical and mechanical properties of the geogrid exert a substantial influence on the flexural performance of the reinforced beams. Additionally, it is worth noting to highlight that the concrete beams reinforced with fibreglass geogrid maintained their structural integrity even when they reached the point of total failure. This starkly contrasts with the control beams, which experienced immediate brittle failure and separation.

5 Acknowledgements

The authors of this study wish to express their gratitude to NSERC and McGill University for their gracious financial support, which significantly contributed to the success of this research endeavour. Additionally, the authors would like to extend their appreciation to their industrial collaborator, Titan Environmental Containment Ltd., for generously supplying the geogrid material, offering valuable technical guidance, and providing financial assistance. A special acknowledgment is reserved for the dedicated technicians at the McGill University laboratory for their invaluable assistance in facilitating access to the laboratory facilities and testing equipment. Lastly, the authors would like to recognize the valuable contributions of graduate student Romaric Desbrousses and undergraduate students Yeshvin Goodary, Jiahao Xu and Evelyn Zhang during their participation in laboratory work.

References

1. Tang, X., Chehab, G.R., Kim, S.: Laboratory study of geogrid reinforcement in Portland cement concrete. *Pavement Crack. Mech. Model. Detect. Test. Case Hist.* 769–778 (2008). <https://doi.org/10.1201/9780203882191.ch75>
2. El Meski, F., Chehab, G.R.: Flexural behavior of concrete beams reinforced with different types of geogrids. *J. Mater. Civ. Eng.* 26, 04014038 (2014). [https://doi.org/10.1061/\(asce\)mt.1943-5533.0000920](https://doi.org/10.1061/(asce)mt.1943-5533.0000920)
3. Pavithra, S., Tamil Selvi, M.: Experimental Study on Application of Geogrid in Concrete to Improve Its Flexural Strength. *Lect. Notes Civ. Eng.* 179, 1–8 (2022). https://doi.org/10.1007/978-981-16-5041-3_1
4. Al Basiouni Al Masri, Z., Daou, A., Haj Chhade, R., Chehab, G.: Experimental and Numerical Assessment of the Behavior of Geogrid-Reinforced Concrete and Its Application in Concrete Overlays. *J. Mater. Civ. Eng.* 30, (2018). [https://doi.org/10.1061/\(asce\)mt.1943-5533.0002542](https://doi.org/10.1061/(asce)mt.1943-5533.0002542)
5. Itani, H., Saad, G., Chehab, G.: The use of geogrid reinforcement for enhancing the performance of concrete overlays: An experimental and numerical assessment. *Constr. Build. Mater.* 124, 826–837 (2016). <https://doi.org/10.1016/j.conbuildmat.2016.08.013>
6. Al-Hedad, A.S.A., Hadi, M.N.S.: Effect of geogrid reinforcement on the flexural behaviour of concrete pavements. *Road Mater. Pavement Des.* 20, 1005–1025 (2019). <https://doi.org/10.1080/14680629.2018.1428217>
7. RajeshKumar, K., Awoyera, P.O., Shyamala, G., Kumar, V., Gurumoorthy, N., Kayikci, S., Romero, L.M.B., Prakash, A.K.: Structural Performance of Biaxial Geogrid Reinforced Concrete Slab. *Int. J. Civ. Eng.* 0123456789, (2021). <https://doi.org/10.1007/s40999-021-00668-y>
8. Al-Hedad, A.S.A., Bambridge, E., Hadi, M.N.S.: Influence of geogrid on the drying shrinkage performance of concrete pavements. *Constr. Build. Mater.* 146, 165–174 (2017). <https://doi.org/10.1016/j.conbuildmat.2017.04.076>
9. ASTM C39/C39M: Standard Test Method for Compressive Strength of Cylindrical Concrete Specimens 1. *ASTM Stand. B. i*, 1–5 (2003)
10. C496/C496M, A.: Standard Test Method for Splitting Tensile Strength of Cylindrical Concrete Specimens. *Man. Hydrocarb. Anal.* 6th Ed. 545-545–3 (2008). <https://doi.org/10.1520/mnl10913m>
11. Shokr, M., Meguid, M.A., Bhat, S.: Experimental Investigation of the Tensile Response of Stiff Fiberglass Geogrid Under Varying Temperatures. *Int. J. Geosynth. Gr. Eng.* 8, (2022). <https://doi.org/10.1007/s40891-022-00361-7>
12. ASTM: Standard test method for flexural strength of concrete (using simple beam with third-point loading) C78/C78M-10. , West Conshohocken, Conshohocken, PA (2015)
13. Çağlar, Y., Şener, S.: Size effect tests of different notch depth specimens with support rotation measurements. *Eng. Fract. Mech.* 157, 43–55 (2016). <https://doi.org/10.1016/j.engfracmech.2016.02.028>
14. Hoover, C.G., Bažant, Z.P.: Universal Size-Shape Effect Law Based on Comprehensive Concrete Fracture Tests. *J. Eng. Mech.* 140, 473–479 (2014). [https://doi.org/10.1061/\(asce\)em.1943-7889.0000627](https://doi.org/10.1061/(asce)em.1943-7889.0000627)
15. Recommendation, R.D.: Determination of the fracture energy of mortar and concrete by means of three-point bend tests on notched beams. *Mater. Struct.* 18, 285–290

- (1985)
16. Guan, J., Hu, X., Wang, Y., Li, Q., Wu, Z.: Effect of fracture toughness and tensile strength on fracture based on boundary effect theory. *J. Hydraul. Eng.* 47, 1298–1306 (2016)
 17. Wang, J.J., Tao, M.X., Nie, X.: Fracture energy-based model for average crack spacing of reinforced concrete considering size effect and concrete strength variation. *Constr. Build. Mater.* 148, 398–410 (2017). <https://doi.org/10.1016/j.conbuildmat.2017.05.082>
 18. Xu, P., Ma, J., Zhang, M., Ding, Y., Meng, L.: Fracture Energy Analysis of Concrete considering the Boundary Effect of Single-Edge Notched Beams. *Adv. Civ. Eng.* 2018, (2018). <https://doi.org/10.1155/2018/3067236>
 19. Sümer, Y., Aktaş, M.: Defining parameters for concrete damage plasticity model. *Chall. J. Struct. Mech.* 1, 149–155 (2015). <https://doi.org/10.20528/cjsmec.2015.07.023>
 20. Al-Rifaie, H., Mohammed, D.: Comparative Assessment of Commonly Used Concrete Damage Plasticity Material Parameters. *Eng. Trans.* 70, 157–181 (2022). <https://doi.org/10.24423/EngTrans.1645.20220613>
 21. Lubliner, J., Oliver, J., Oller, S., Oñate, E.: A plastic-damage model for concrete. *Int. J. Solids Struct.* 25, 299–326 (1989). [https://doi.org/10.1016/0020-7683\(89\)90050-4](https://doi.org/10.1016/0020-7683(89)90050-4)
 22. Lee, J., Fenves, G.L.: Plastic-damage model for cyclic loading of concrete structures. *J. Eng. Mech.* 124, 892–900 (1998)
 23. 318, A.C.I.C.: Building code requirements for structural concrete : (ACI 318-95) ; and commentary (ACI 318R-95). Farmington Hills, MI: American Concrete Institute, [1995] ©1995
 24. Zinkaah, O.H., Alridha, Z., Alhawat, M.: Numerical and theoretical analysis of FRP reinforced geopolymer concrete beams. *Case Stud. Constr. Mater.* 16, e01052 (2022). <https://doi.org/10.1016/j.cscm.2022.e01052>
 25. Tao, Z., Wang, Z. Bin, Yu, Q.: Finite element modelling of concrete-filled steel stub columns under axial compression. *J. Constr. Steel Res.* 89, 121–131 (2013). <https://doi.org/10.1016/j.jcsr.2013.07.001>
 26. Temsah, Y., Jahami, A., Khatib, J., Sonebi, M.: Numerical analysis of a reinforced concrete beam under blast loading. *MATEC Web Conf.* 149, 02063 (2018). <https://doi.org/10.1051/mateconf/201814902063>
 27. Raza, A., Khan, Q.U.Z., Ahmad, A.: Numerical investigation of load-carrying capacity of GFRP-reinforced rectangular concrete members using CDP model in abaqus. *Adv. Civ. Eng.* 2019, (2019). <https://doi.org/10.1155/2019/1745341>
 28. Manual, A.U.: Version 6.8, Hibbit, Karls-son & Sorensen. Inc., Pawtucket, Rhode Island, USA. (2008)
 29. Genikomsou, A.S., Polak, M.A.: Finite element analysis of punching shear of concrete slabs using damaged plasticity model in ABAQUS. *Eng. Struct.* 98, 38–48 (2015). <https://doi.org/10.1016/j.engstruct.2015.04.016>
 30. Lee, S.H., Abolmaali, A., Shin, K.J., Lee, H. Du: ABAQUS modeling for post-tensioned reinforced concrete beams. *J. Build. Eng.* 30, 101273 (2020). <https://doi.org/10.1016/j.jobbe.2020.101273>
 31. Bencardino, F., Condello, A.: SRG / SRP – concrete bond – slip laws for externally strengthened RC beams. 132, 804–815 (2015). <https://doi.org/10.1016/j.compstruct.2015.06.068>

32. Ibrahim, A.M.A., Fahmy, M.F.M., Wu, Z.: 3D finite element modeling of bond-controlled behavior of steel and basalt FRP-reinforced concrete square bridge columns under lateral loading. *Compos. Struct.* 143, 33–52 (2016). <https://doi.org/10.1016/j.compstruct.2016.01.014>
33. Elchalakani, M., Karrech, A., Dong, M., Mohamed Ali, M.S., Yang, B.: Experiments and Finite Element Analysis of GFRP Reinforced Geopolymer Concrete Rectangular Columns Subjected to Concentric and Eccentric Axial Loading. *Structures*. 14, 273–289 (2018). <https://doi.org/10.1016/j.istruc.2018.04.001>
34. Gouda, O., Asadian, A., Galal, K.: Flexural and Serviceability Behavior of Concrete Beams Reinforced with Ribbed GFRP Bars. *J. Compos. Constr.* 26, 1–19 (2022). [https://doi.org/10.1061/\(asce\)cc.1943-5614.0001253](https://doi.org/10.1061/(asce)cc.1943-5614.0001253)
35. Raza, A., Ahmad, A.: Numerical investigation of load-carrying capacity of GFRP-reinforced rectangular concrete members using CDP model in ABAQUS. *Adv. Civ. Eng.* 2019, (2019)